vulcanhammer.info
March 2022


DOI: 10.13140/RG.2.2.30074.36805

# Inclusion of Rotational Inertial Effects in Power Consumption Calculations for Vibratory Pile Equipment

Don C. Warrington, Ph.D., P.E.
University of Tennessee at Chattanooga
Department of Mechanical Engineering

Virtually all treatments of power consumption and modelled performance for vibratory pile driving equipment assume a constant rotational speed of the eccentrics. In reality this is not possible due to the inertial effects of the eccentrics themselves and the necessity that, without inertia, the power output of the motor for the eccentrics must follow the instantaneous power requirements, which continuously vary. In this paper the rotational inertial effects of the eccentrics are included in the calculations. Because of the non-linear nature of the equations, a numerical model was developed to estimate the dimensionless torque required to turn the eccentrics at a target rotational speed. The results track closely with those of the continuous torque model described by Warrington (2006) for a wide variety of inertia/eccentric moment ratios, although there are exceptional cases if the peak acceleration is increased and the frequency decreased. As an excursus, the method of computing the inertia/eccentric moment ratio and its corresponding pendulum frequency is described in detail for those who can apply this to other problems.

*Keywords:* vibratory pile drivers, power requirements, torque, mass moment of inertia, area moment of inertia

## Introduction

It is difficult to argue with the following, from Verstov and Judina (2015):

> Modern technologies of using vibration during construction have become possibly due, mainly, to Russian researcher and engineers...Results of such researches were the basis for foreign construction vibration technologies. The most illustrious example is vibration technology for inserting and extracting pipes and dowels. Theoretical and experimental research of this process was carried out in Russia during 1930s and 1940s; during 1950s vibration-plungers became widely used for construction works. Foreign companies began manufacturing vibration machines only during 1960s...

The end of the initial research on this topic for both vibratory and impact-vibration hammers, which took place before the end of the Soviet era, left many "loose ends" in our understanding of the technology. (For a description of the physical setup of vibratory pile driving equipment, see Warrington (1992).) One of those "loose ends" is the assumption that rotational speed is constant. Variations in torque experienced by the eccentrics make this impossible unless either a) the torque matches the moment load on the eccentrics at all times, or b) the rotational inertia of the eccentrics is infinite. Neither of these conditions is realistic.

Inclusion of the rotational inertia of the eccentrics (and with them the parts that rotate with them) and elimination of the assumption of constant rotational velocity adds significant complexity to the system. The average rotational velocity (assuming a sinusoidal "ripple" in this quantity) becomes the result of the load on the system and the torque applied against the load. Alternatively the average rotational velocity can be made a target and the torque varied, which is the approach that will generally be taken in this paper.

## Development of the Governing Equations

The governing equations developed here are modified from those of Tseitlin, Verstov, and Azbel (1987) as applied to impact-vibration hammers. They are as follows:

$$I_o \frac{d^2}{dt^2}\alpha(t) = T + K\cos(\alpha(t))\frac{d^2}{dt^2}x(t) \tag{1}$$

I would like to thank two people. The first is Dr. K. Rainer Massarsch of Geo Risk & Vibration Scandinavia AB, whose interest and support of this work has been crucial to its restart. The second is Dr. Boris Belinskiy of the University of Tennessee at Chattanooga, whose help with the governing equations has also been crucial to their successful solution.

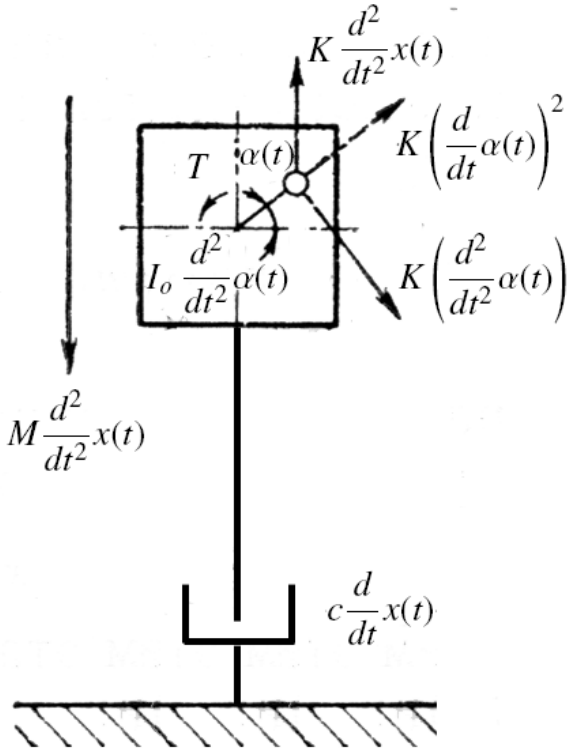


*Figure 1*. Schematic of vibrating system with damping as the ground resistance (modified from Tseitlin et al. (1987))

$$M\frac{d^2}{dt^2}x(t) = -c\frac{d}{dt}x(t) - K\left(\frac{d}{dt}\alpha(t)\right)^2\sin(\alpha(t)) + K\left(\frac{d^2}{dt^2}\alpha(t)\right)\cos(\alpha(t)) \tag{2}$$

The system is shown schematically in Figure 1.

These equations differ from Tseitlin et al. (1987) in the following ways:

1. The spring system is eliminated and the load is replaced by damping $c$. Use of constant damping to simulate the resistance of the soil to vibration has been done for many years for estimating torque and power requirements (Erofeev, Smorodinov, Fedorov, Vyazovkii, and Villumsen (1985); Warrington (1994, 2006).)

2. All effects due to gravity are eliminated. Although gravity is an important component in vibratory systems, its elimination is primarily for making reasonable comparisons to fixed-speed models such as Warrington (2006), where it does not appear.

3. For our purposes the torque $T$ is assumed to be constant.

Performing algebra and rearrangement, this yields

$$\frac{d^2}{dt^2}\alpha(t) - \frac{K\cos(\alpha(t))\frac{d^2}{dt^2}x(t)}{I_o} = \frac{T}{I_o} \tag{3}$$

$$-\frac{K\left(\frac{d^2}{dt^2}\alpha(t)\right)\cos(\alpha(t))}{M} + \frac{d^2}{dt^2}x(t) = -\frac{c\frac{d}{dt}x(t)}{M} - \frac{K\left(\frac{d}{dt}\alpha(t)\right)^2\sin(\alpha(t))}{M} \tag{4}$$

The scheme of rearrangement will be explained shortly.

At this point the first variable change is made

$$\tau = \omega_0\, t \tag{5}$$

which results in

$$\omega_0{}^2\frac{d^2}{d\tau^2}\alpha(\tau) - \frac{K\cos(\alpha(\tau))\omega_0{}^2\frac{d^2}{d\tau^2}x(\tau)}{I_o} = \frac{T}{I_o} \tag{6}$$

$$-\frac{K\omega_0{}^2\left(\frac{d^2}{d\tau^2}\alpha(\tau)\right)\cos(\alpha(\tau))}{M} + \omega_0{}^2\frac{d^2}{d\tau^2}x(\tau) = -\frac{\omega_0\, c\frac{d}{d\tau}x(\tau)}{M} - \frac{K\omega_0{}^2\left(\frac{d}{d\tau}\alpha(\tau)\right)^2\sin(\alpha(\tau))}{M} \tag{7}$$

At this point the second variable change is made by defining

$$\omega_0 = \sqrt{\frac{K g_c}{I_o}} \tag{8}$$

This is the "pendulum frequency" of the eccentrics, the frequency at which the eccentrics "rock" when moved a small angle. Although it may not seem very useful when first presented, it makes further simplification of the equations possible, although there are challenges to using this frequency. Doing this yields

$$g_c\,\omega_0{}^2\frac{d^2}{d\tau^2}\alpha(\tau) - \omega_0{}^4\cos(\alpha(\tau))\frac{d^2}{d\tau^2}x(\tau) = \frac{\omega_0{}^2 T}{K} \tag{9}$$

$$-\frac{K\omega_0{}^2\left(\frac{d^2}{d\tau^2}\alpha(\tau)\right)\cos(\alpha(\tau))}{g_c\, M} + \frac{\omega_0{}^2\frac{d^2}{d\tau^2}x(\tau)}{g_c} = -\frac{\omega_0\, c\frac{d}{d\tau}x(\tau)}{g_c\, M} - \frac{K\omega_0{}^2\left(\frac{d}{d\tau}\alpha(\tau)\right)^2\sin(\alpha(\tau))}{g_c\, M} \tag{10}$$

At this point the third variable change is made

$$X(\tau) = \frac{x(\tau)\omega_0{}^2}{g_c} \tag{11}$$

which results in the following

$$\frac{d^2}{d\tau^2}\alpha(\tau) - \cos(\alpha(\tau))\frac{d^2}{d\tau^2}X(\tau) = \frac{T}{g_c\, K} \tag{12}$$

$$-\frac{K\omega_0{}^2\left(\frac{d^2}{d\tau^2}\alpha(\tau)\right)\cos(\alpha(\tau))}{g_c\, M} + \frac{d^2}{d\tau^2}X(\tau) = -\frac{c\frac{d}{d\tau}X(\tau)}{\omega_0\, M} - \frac{K\omega_0{}^2\left(\frac{d}{d\tau}\alpha(\tau)\right)^2\sin(\alpha(\tau))}{g_c\, M} \tag{13}$$

Finally three constants are defined as follows:

$$\eta_1 = \frac{T}{g_c\, K} \tag{14}$$

$$\eta_2 = \frac{c}{M\omega_0} \tag{15}$$

$$\eta_3 = \frac{K{\omega_0}^2}{Mg_c} \tag{16}$$

and at last

$$\frac{d^2}{d\tau^2}\alpha(\tau) - \cos(\alpha(\tau))\frac{d^2}{d\tau^2}X(\tau) = \eta_1 \tag{17}$$

$$-\eta_3\left(\frac{d^2}{d\tau^2}\alpha(\tau)\right)\cos(\alpha(\tau)) + \frac{d^2}{d\tau^2}X(\tau) = -\eta_2\frac{d}{d\tau}X(\tau) - \eta_3\left(\frac{d}{d\tau}\alpha(\tau)\right)^2\sin(\alpha(\tau)) \tag{18}$$

## Issues Surrounding the Governing Equations

### Computation of the Rotational Inertia, Eccentric Moment and Their Ratio

In Equations 17 and 18, the rotational inertia $I_o$ does not appear independently, but only through the pendulum frequency $\omega_0$ and in conjunction with the eccentric moment $K$. Defining

$$I_K = \frac{I_o}{K} \tag{19}$$

then Equation 8 becomes

$$\omega_0 = \sqrt{\frac{g_c}{I_K}} \tag{20}$$

There is thus a one-to-one transformation assuming $\omega_o > 0$.

Determination of the eccentric moment is routine with vibratory pile drivers as it is a key specification. Determination of the rotational inertia is not so common, and from a practical standpoint it is complicated by the fact that the area moment of inertia is much more readily tabulated than the mass moment of inertia $I_o$. However, with the configuration of many vibratory machines, the area moment can be used to determine this ratio. To accomplish this the following assumptions are made:

1. Only the polar or rotational moment of inertia around the axis of rotation is considered, which in this case is the moment of inertia (area or mass) of interest.

2. All of the components are of uniform thickness in the $z$ axis, the axis about which the components rotate. This is commonly true with vibratory components such as eccentrics, gears and shafts.

3. All of the components are made of the same material with the same density $\rho$. This is true for many vibratory hammers. Notable exceptions are those with tungsten inserts, as opposed to all-steel construction. Eliminating this assumption would complicate the mathematics somewhat but it is the least important of the assumptions.

With these assumptions, the polar mass moment of inertia can be expressed by the equation (Meriam (1975))

$$I_o = \rho\, t_1 J_o \tag{21}$$

The eccentric moment for such a component is

$$K = \rho\, t_1 A C_G \tag{22}$$

Applying Equations 21 and 22 to Equation 19 yields

$$I_K = \frac{J_o}{AC_G} \tag{23}$$

from which the pendulum frequency can be computed using Equation 20. Defining an "eccentric area"

$$K_{area} = AC_G \tag{24}$$

Equation 23 reduces to

$$I_K = \frac{J_o}{K_{area}} \tag{25}$$

As an example, consider a simple semicircular mass which rotates about the mid-point of the flat side. The area moment of inertia around the rotation axis is

$$J_o = \frac{\pi r^4}{4} \tag{26}$$

The "area eccentric moment" is the product of the distance from the centre of gravity and the cross-sectional area of the semicircle

$$K_{area} = 2/3\, r^3 \tag{27}$$

The ratio of the moment of inertia to the eccentric moment is, from Equation 25,

$$I_K = 3/8\, r\pi \approx 1.18r \tag{28}$$

Considering, for example, semicircles mounted into Vulcan vibratory hammers with a maximum radius of 19 cm, $I_K = 22.48\, cm$ and $\omega_0 = 6.61\ {}^{rad}/_{sec}$ or $RPM_0 = 63\, RPM$.

For situations where there are different thicknesses of the components, it can be shown that $I_K$ can be determined as follows

$$I_K = \frac{\sum_{i=1}^{m} \rho\, t_i J_{oi}}{\sum_{i=1}^{m} \rho\, t_i K_{areai}} \tag{29}$$

Unless the eccentrics are composite in material, or there are varying materials in the components, the $\rho$ term can be divided out of the equation. With homogeneous eccentrics, there is usually only one non-zero term in the denominator.

As a very brief survey of existing equipment, two examples were considered. One is the Foster 1000 vibratory, a machine with a conventional gear/eccentric/shaft arrangement, with the gears and eccentrics connected to the shaft

Table 1
*Sample Values of Inertia-Eccentric Moment Ratio and Frequencies*

| Machine | $I_K$, cm | $\omega_o$, rad/sec | $RPM_0$ |
|---|---|---|---|
| "Vulcan" Semicircle | 22.5 | 6.61 | 63 |
| Vulcan 1400 (l/arch ring) | 30.7 | 5.65 | 54 |
| Foster 1000 | 47.8 | 4.53 | 43.3 |
| Vulcan 1400 (w/arch ring) | 90.1 | 3.3 | 31.5 |

and each other. The second is a Vulcan 1400, which used a thick plate with the eccentric moment burned out of the plate. As a result of this there is a semicircular arch for the gears to mesh at all angles. In the eccentric area the arch continues, thus forming an 'arch ring' around the eccentric. Equation 29 was applied and the results are shown in Table 1.

Based on this, it was decided to consider a range of values $20 \leq RPM_0 \leq 200$.

**Defining the Constants in the Equations of Motion**

Equations 17 and 18 have three constants which must be evaluated (or at least have ranges of values to evaluate.) These can be related to similar quantities as described by Warrington (1994, 2006).

The first, $\eta_1$, is the exact equivalent of the torque ratio $T_r$, the ratio of the motor torque to the eccentric moment,

$$T_r = \eta_1 \tag{30}$$

Since the effect of including the rotational inertia is initially unknown, determining this ratio is a central object of the study.

The second and third, $\eta_2$ and $\eta_3$, are analogous to the damping coefficient $\zeta$[1] and the free-hanging peak acceleration $n$ respectively, given by the equations

$$\zeta = \frac{c}{M\omega_1} \tag{31}$$

$$n = \frac{K\omega_1^2}{Mg_c} \tag{32}$$

By "analogous" it means that the form of the constants is the same but that the frequency they are based on is different. Comparison of the result of the semi-circle and frequencies vibratory pile drivers normally operate at will show the disparity between the two. Since the "base" frequency of these equations is the pendulum frequency and not the frequency of rotation (which is to be determined,) these values need to be expressed in terms of the pendulum frequency.

To solve this problem, defining

$$\omega_{rat} = \frac{\omega_1}{\omega_0} = \frac{RPM_1}{RPM_0} \tag{33}$$

and using this, the values of $\eta_2$ and $\eta_3$ can be computed as follows

$$\eta_2 = \zeta\omega_{rat} \tag{34}$$

$$\eta_3 = \frac{n}{\omega_{rat}^2} \tag{35}$$

**Solution Technique for the Governing Equations**

The non-linear nature of Equations 17 and 18 virtually precludes a closed-form solution. It is necessary to utilise a numerical solution. That numerical solution is in two parts:

1. Solution of the equations themselves, using a fourth-order Runge-Kutta technique. At the beginning values of $\eta_2$ and $\eta_3$ are assumed with initial input of $\omega_0$ and an initially assumed $\omega_1$. The result for an input value of $\eta_1$ is an operating frequency $\omega_1$, which may or may not coincide with that assumed initially.

2. A regula falsi method is employed which varies the value of $\eta_1$ until the final result of $\omega_1$ is within an acceptable bound of the originally assumed $\omega_1$ is achieved.

Both of these methods are described in Carnahan, Luther, and Wilkes (1969), from whence the code was taken.

To set up the Runge-Kutta Method, which requires a series of first derivatives, the following are defined:

$$\begin{aligned} Y_1 &= \alpha(\tau) \\ Y_2 &= \frac{d}{d\tau}\alpha(\tau) \\ Y_3 &= X(\tau) \\ Y_4 &= \frac{d}{d\tau}X(\tau) \end{aligned} \tag{36}$$

and

$$\begin{aligned} F_1 &= Y_2 \\ F_2 &= \frac{d^2}{d\tau^2}\alpha(\tau) \\ F_3 &= Y_4 \\ F_4 &= \frac{d^2}{d\tau^2}X(\tau) \end{aligned} \tag{37}$$

The governing equations can thus be expressed as

$$F_2 - \cos(Y_1)F_4 = \eta_1 \tag{38}$$

$$-\eta_3 F_2 \cos(Y_1) + F_4 = -\eta_2 Y_4 - \eta_3 {Y_2}^2 \sin(Y_1) \tag{39}$$

[1] In Warrington (2006) this variable is referred to as $\tau$, but to prevent confusion the nomenclature for Warrington (1994) is used.

The second derivative terms were shifted to the left hand side (Equations 3 and 4) to make it possible to put the equations into $Ax = b$ matrix form, thus

$$A = \begin{bmatrix} 1 & -\cos(Y_1) \\ -\eta_3 \cos(Y_1) & 1 \end{bmatrix} \tag{40}$$

$$x = \begin{bmatrix} F_2 \\ F_4 \end{bmatrix} \tag{41}$$

$$b = \begin{bmatrix} \eta_1 \\ -\eta_2 Y_4 - \eta_3 {Y_2}^2 \sin(Y_1) \end{bmatrix} \tag{42}$$

Inverting $A$ and solving for $x$, at last

$$\begin{bmatrix} F_2 \\ F_4 \end{bmatrix} = \begin{bmatrix} -\frac{\eta_1}{-1+(\cos(Y_1))^2\eta_3} - \frac{\cos(Y_1)\left(-\eta_2 Y_4 - \eta_3 {Y_2}^2 \sin(Y_1)\right)}{-1+(\cos(Y_1))^2\eta_3} \\ -\frac{\eta_3 \cos(Y_1)\eta_1}{-1+(\cos(Y_1))^2\eta_3} - \frac{-\eta_2 Y_4 - \eta_3 {Y_2}^2 \sin(Y_1)}{-1+(\cos(Y_1))^2\eta_3} \end{bmatrix} \tag{43}$$

This can be substituted into Equation 37 and used in the integration.

## Initial Results and Analysis

With the model constructed, the following parameters were determined for the initial analysis:

1. Target RPM was set at $RPM_1 = 1600$. The bracket values of $T_r$ were initially set at 1 and 10.

2. Based on Warrington (2006), $\zeta = 1$ and $n = 9$.

3. The range of pendulum frequencies is, as noted earlier, $20 \leq RPM_0 \leq 200$.

With all this, the initial results were surprising. The values of $T_r = 2.25$ within numerical accuracy. Only when the pendulum frequency approached the upper limit did this begin to vary from this result, and even then within 1%. The model began to have more difficulty achieving the target RPM at higher pendulum frequencies.

In an attempt to understand this, it is necessary to note that the instantaneous torque predicted by constant rotational speed theory is (Warrington (2006))

$$T_{inst} = 1/2 \, \frac{K^2 {\omega_1}^2 \left(\sin(2\,\omega_1\, t) + \zeta \, \left(\cos(2\,\omega_1\, t) + 1\right)\right)}{M\left(\zeta^2 + 1\right)} \tag{44}$$

Defining, in a manner similar to Equation 5,

$$\tau_1 = \omega_1 t \tag{45}$$

the instantaneous torque ratio is (employing Equations 14, 30 and 32)

$$T_{r_{inst}} = 1/2 \, \frac{n\left(\sin(2\,\tau_1) + \zeta \, \cos(2\,\tau_1) + \zeta\right)}{\zeta^2 + 1} \tag{46}$$

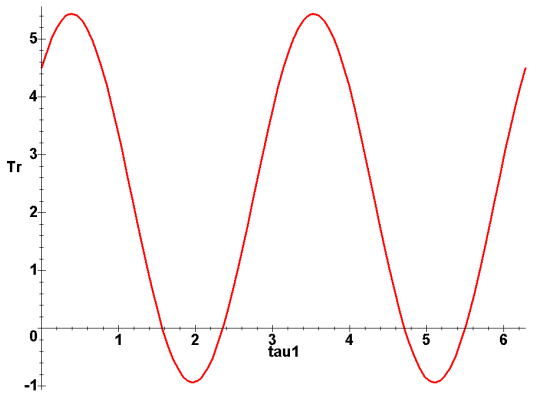


*Figure 2.* Plot of Equation 46 with $n = 9$ and $\zeta = 1$ for $0 \leq \tau_1 \leq 2\pi$

A plot of Equation 46 is shown in Figure 2. This plot shows the constant changing of the torque which is characteristic of vibrating pile driving systems.

Integrating this over a complete cycle $2\pi$ and then divide it by the period, the average torque ratio is

$$T_{r_{avg}} = 1/2 \, \frac{n\zeta}{\zeta^2 + 1} \tag{47}$$

From this the following:

1. The maximum value of $T_{r_{avg}}$ takes place when $\zeta = 1$, which is consistent with Warrington (1994).

2. Substituing this value and $n = 9$, the result is $T_{r_{avg}} = \frac{9}{4} = 2.25$, which is consistent with our numerical model.

For this range of input parameters, it can be concluded that the effect of changing the mass moment of inertia is minimal, at least for the ranges of ordinary vibratory pile driving equipment.

That being the case, perhaps this is the occasion to discuss the unsatisfactory state of affairs described in Warrington (2006) concerning the relationships between the torque ratio and the power coefficient $\alpha_N$, given by the equation

$$N = \frac{\alpha_N \, K^2 {\omega_1}^3}{M} \tag{48}$$

From Equation 47, the power can be computed by the equation (with substitutions from Equations 30 and 32

$$N = T\omega_1 = 1/2 \, \frac{n\zeta \, K g_c \, \omega_1}{\zeta^2 + 1} \tag{49}$$

Equating these two and solving for $\alpha_N$,

$$\alpha_N = 1/2 \, \frac{\zeta}{\zeta^2 + 1} \tag{50}$$

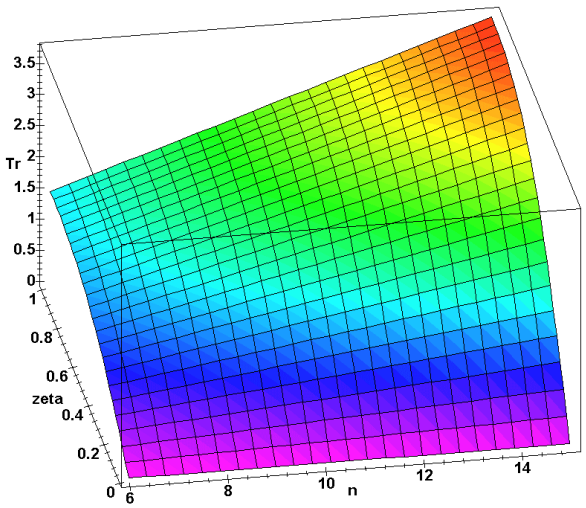


*Figure 3.* Variation of Torque Ratio with Free-Hanging Acceleration and Damping Coefficient, Constant Angular Velocity

The maximum value of $\alpha_N$ takes place when $\zeta = 1$, and $\alpha_N = \frac{1}{4}$, as one would expect.

It is noteworthy that $\alpha_N$ is independent of $n$; however, the power required is not. Equation 48 can be rewritten as

$$N = \alpha_N K \omega_1 n g_c \tag{51}$$

For a given machine with a given eccentric moment and rotational velocity, if the value of $n$ is increased, the power must be also. Equations 47 and 51 can be combined to obtain the relationship between the torque ratio and $\alpha_N$,

$$T_{r_{avg}} = n\alpha_N \tag{52}$$

Equation 52 suggests that the value of peak acceleration $n$ should be varied in parametric studies of the inertial model. Equation 52 also shows that the relationship shown in Warrington (2006) between $\alpha_N$ and $T_{r_{avg}}$ for design purposes is either generous in power loss estimation, implicitly assumes $n > 9$, or both, and is in any case conservative.

## Detailed Results and Analysis

The initial results indicated that the inclusion of inertial effects (within the range under study) would yield results that would track closely with those obtained with constant angular velocity theory. That being the case, it was decided to use the latter as a baseline and determine the variation of the results of the inertial model from that baseline.

To do this, the variation of torque ratio $T_r$ with peak free-hanging acceleration $n$ and damping coefficient $\zeta$ (determined from Equation 47) is shown in Figure 3.

From here, the simplest way to compare the result of the inertial model with the constant velocity values is to plot the

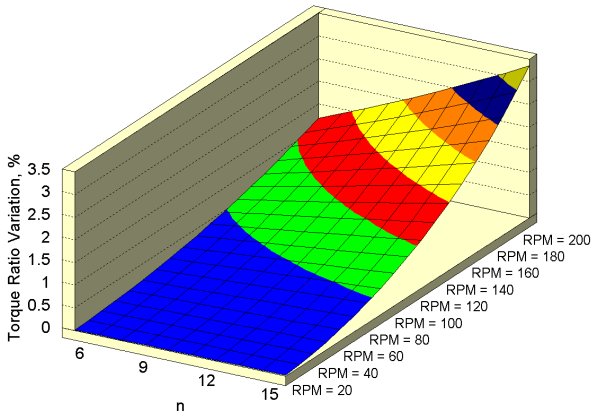


*Figure 4.* Values of Torque Ratio Variation as a Function of $n$ and $RPM_0$ for $\zeta = \frac{1}{4}$ and $RPM_1 = 1600\,RPM$

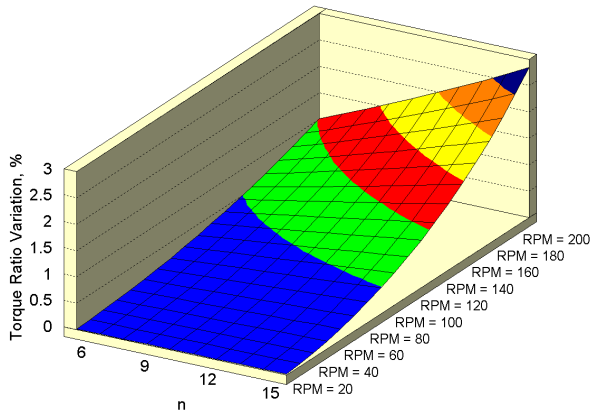


*Figure 5.* Values of Torque Ratio Variation as a Function of $n$ and $RPM_0$ for $\zeta = \frac{1}{2}$ and $RPM_1 = 1600\,RPM$

percentage difference between the two for a) various values of $RPM_0$ and $n$ and b) $RPM_1 = 1600\,RPM$. This was done for values of $\zeta = \frac{1}{4}, \frac{1}{2}, \frac{3}{4}$ and 1. The results are shown for these values in Figures 4, 5, 6 and 7 respectively.

The pattern in all of these is the same; the variation from constant velocity theory is smallest with the lowest pendulum frequency (largest relative inertia to eccentric moment) and increases until it is at the maximum with increasing pendulum frequency and peak free-hanging acceleration. Looking at all four figures also shows that the variation decreases with increasing values of $\zeta$. However, even with the smallest analysed values of $\zeta$, the variation is small, no greater than 3.5%. For this rotational speed, if the pendulum frequency can be restricted to $RPM_0 \leq 80\,{}^{rev}/_{min}$, the variation of the torque ratio from constant angular velocity theory is less than around 0.5%.

The same series of data points are run for $RPM_1 = 2400\,RPM$, and the results are shown for values of $\zeta = \frac{1}{4}, \frac{1}{2}, \frac{3}{4}$ and 1 in Figures 8, 9, 10 and 11 respectively.

The pattern of $T_r$ relative to $n$ and $RPM_0$ is essentially the

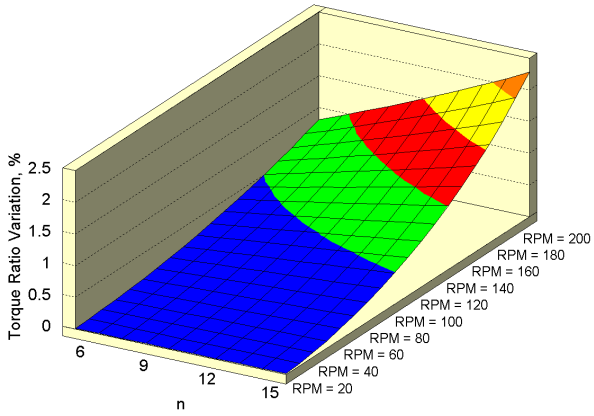


*Figure 6*. Values of Torque Ratio Variation as a Function of $n$ and $RPM_0$ for $\zeta = \frac{3}{4}$ and $RPM_1 = 1600\,RPM$

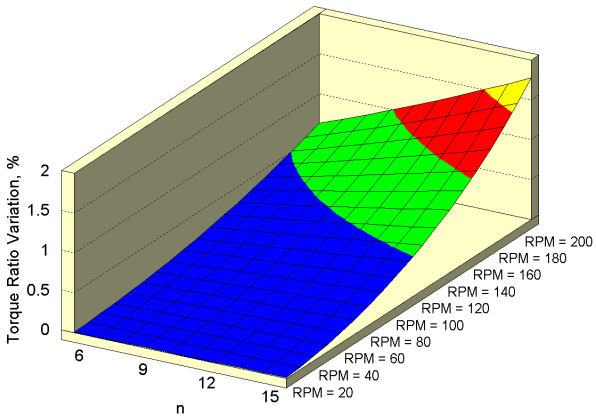


*Figure 7*. Values of Torque Ratio Variation as a Function of $n$ and $RPM_0$ for $\zeta = 1$ and $RPM_1 = 1600\,RPM$

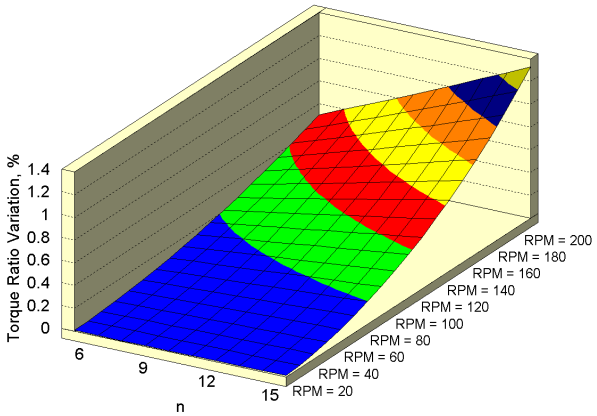


*Figure 8*. Values of Torque Ratio Variation as a Function of $n$ and $RPM_0$ for $\zeta = \frac{1}{4}$ and $RPM_1 = 2400\,RPM$

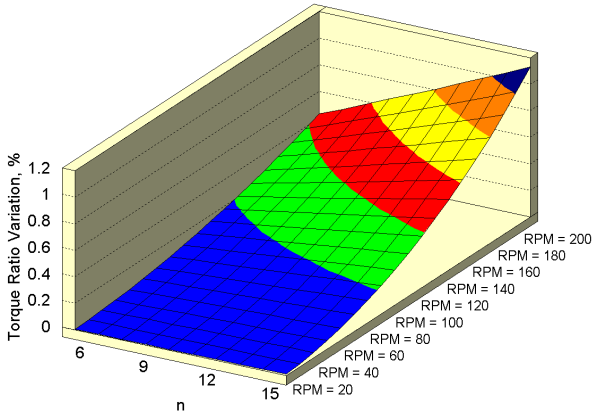


*Figure 9*. Values of Torque Ratio Variation as a Function of $n$ and $RPM_0$ for $\zeta = \frac{1}{2}$ and $RPM_1 = 2400\,RPM$

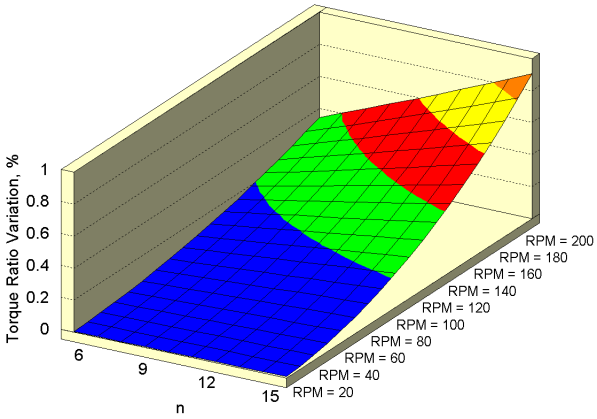


*Figure 10*. Values of Torque Ratio Variation as a Function of $n$ and $RPM_0$ for $\zeta = \frac{3}{4}$ and $RPM_1 = 2400\,RPM$

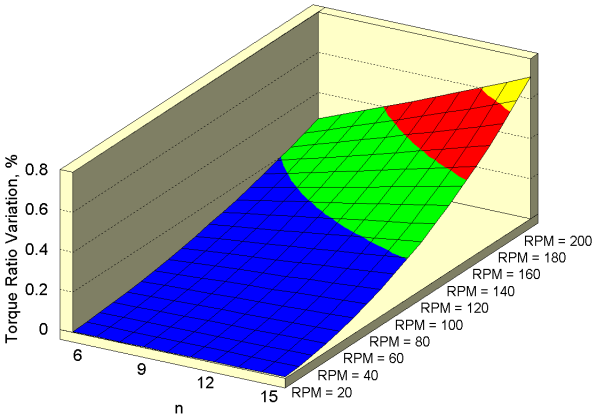


*Figure 11*. Values of Torque Ratio Variation as a Function of $n$ and $RPM_0$ for $\zeta = 1$ and $RPM_1 = 2400\,RPM$

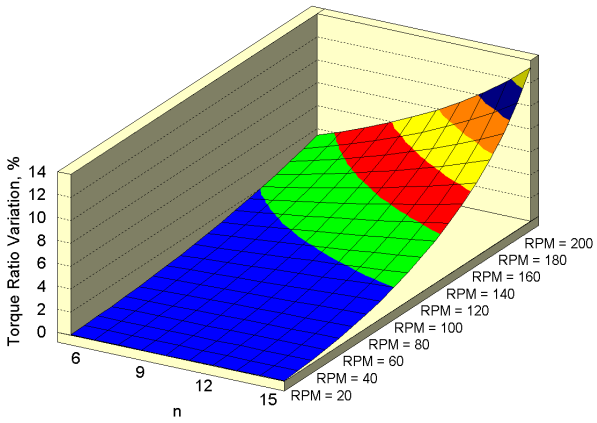


*Figure 12*. Values of Torque Ratio Variation as a Function of $n$ and $RPM_0$ for $\zeta = \frac{1}{4}$ and $RPM_1 = 1000\,RPM$

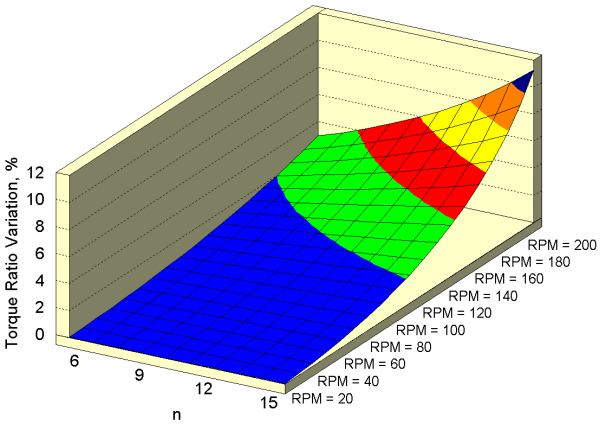


*Figure 13*. Values of Torque Ratio Variation as a Function of $n$ and $RPM_0$ for $\zeta = \frac{1}{2}$ and $RPM_1 = 1000\,RPM$

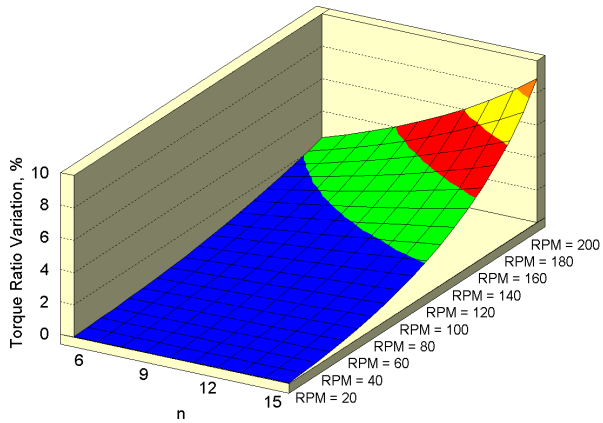


*Figure 14*. Values of Torque Ratio Variation as a Function of $n$ and $RPM_0$ for $\zeta = \frac{3}{4}$ and $RPM_1 = 1000\,RPM$

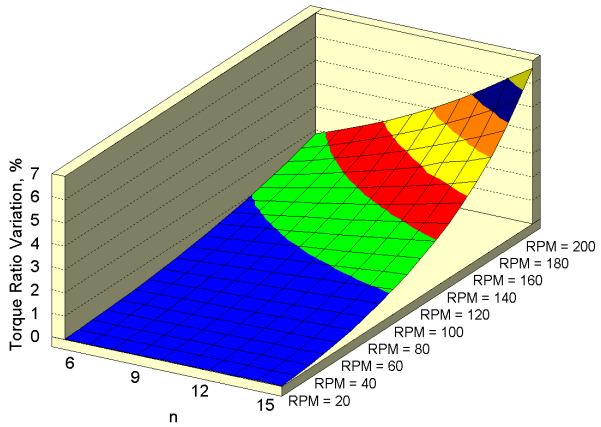


*Figure 15*. Values of Torque Ratio Variation as a Function of $n$ and $RPM_0$ for $\zeta = 1$ and $RPM_1 = 1000\,RPM$

same as was seen with the 1600 RPM cases; however, the overall effect of the inertia of the eccentrics (probably better referred to as the pendulum effect) is less with the higher frequency.

Finally $RPM_1 = 1000\,RPM$ is considered, with results for values of $\zeta = \frac{1}{4}, \frac{1}{2}, \frac{3}{4}$ and 1 in Figures 12, 13, 14 and 15 respectively.

In these cases the variation of torque ratio from the constant angular velocity case is considerably more than the other two cases; in fact, to maintain a maximum torque variance of less than 0.5%, it is necessary to keep the pendulum frequency below 50 RPM, which is considerably less than that for the 1600 RPM cases.

## Discussion

1. The use of a purely velocity-dependent damping model as the soil resistance to vibration has its limitations, especially when toe resistance is taken into consideration, and this can be seen even in the most elementary models of vibratory pile driving (Warrington (2021).) However it is a reasonable guide to torque and power requirements, and in cases where its model is most applicable (sheet piling with limited toe resistance, or possibly compaction) it is very useful.

2. Whether increasing the value of peak acceleration is necessary to induce the types of changes in soil response that occurs with vibratory action is beyond the scope of this study, and doubtless depends upon the application, but if it is done then the power needs to be increased accordingly. It should be noted that increasing the peak acceleration also increases the variation of the torque ratio relative to the constant velocity case. The two effects compound each other, and this needs to be considered in the configuration of the machines.

3. The effect of the pendulum frequency increases as a) the pendulum frequency becomes closer to the operating frequency and b) the peak free-hanging acceleration increases. If, for example, it is necessary to restrict the variation of the torque ratio to 0.5%, the results show that the rotational frequency should be no less than 20 times the pendulum fre-

quency. Whether this criterion can be "loosened" is a decision that is beyond the scope of this paper.

4. In vibratory machines that have power transmitting elements such as pinion gears and shafts and the motor itself, these elements add to the rotational inertia of the system and thus tend to drive the pendulum frequency down from values such as are computed in Table 1.

5. There are other losses in vibratory machines that may be more significant than those described in this paper. These losses would include losses in the hydraulic hoses, quick disconnects and internal valving in the power pack. Electric machines have their own losses to consider. It is possible to include these losses by increasing the value of $\alpha_N$ but there are other ways of doing this, as is discussed in Erofeev et al. (1985).

## Conclusion

Inclusion of inertial effects in modelling vibratory hammer operation result in some increase in the apparent torque requirements of the system from the conventional constant rotational velocity case. For most combinations of operating and pendulum frequency, these are not significant compared with other losses, and the constant $\omega_1$ assumption that has been used for many years in the design of vibratory pile drivers can be used. In some situations, however, these pendulum frequency related losses can be important, and should be considered.

## Nomenclature

| | |
|---|---|
| $\alpha(t)$, $\alpha(\tau)$ | Angle of eccentric, radians |
| $\alpha_N$ | Power factor, dimensionless |
| $\eta_{1,2,3}$ | System constants |
| $\omega$ | Frequency, $^{rad}/_{sec}$ |
| $\omega_0$ | Pendulum frequency, $^{rad}/_{sec}$ |
| $\omega_1$ | Rotational frequency, $^{rad}/_{sec}$ |
| $\omega_{rat}$ | Ratio of Rotational to Pendulum Frequency, dimensionless |
| $\rho$ | Density, $^{kg}/_{m^3}$ |
| $\tau$ | Dimensionless time |
| $\tau_1$ | Dimensioness period of eccentric rotation |
| $\zeta$ | Dimensionless damping factor |
| $A$ | Cross-sectional area of eccentric region, $m^2$ |
| $c$ | Damping from soil, $^{N-sec}/_{m}$ |
| $C_G$ | Distance from centroid of eccentric region to centre of rotation, $m$ |
| $F_{1,2,3,4}$ | Second derivative functions for Runge-Kutta method |
| $g_c$ | Acceleration due to gravity = 9.81 $^{m}/_{sec}$ |
| $I_K$ | Ratio of mass moment of inertia to eccentric moment, m |
| $I_o$ | Mass moment of inertia around the centre of rotation, $kg - m^2$ |
| $J_o$ | Area moment of inertia, $m^4$ |
| $K$ | Eccentric Moment, $kg - m$ |
| $K_{area}$ | Eccentric area, $m^3$ |
| $M$ | Vibrating mass, kg |
| $m$ | Number of elements in rotating system |
| $N$ | Power, W |
| $n$ | Peak free-hanging acceleration, g's |
| $r$ | Radius of semicircle, $m$ |
| $RPM_0$ | Expression of pendulum frequency in $^{rev}/_{min}$ |
| $RPM_1$ | Rotational Frequency, $^{rev}/_{min}$ |
| $T$ | Torque, J |
| $t$ | Time, seconds |
| $T_r$ | Torque ratio, dimensionless |
| $T_{ravg}$ | Average torque ratio |
| $T_{rinst}$ | Instantaneous torque ratio |
| $t_i$ | Thickness of a rotating element, $i = 1, 2, 3...$ |
| $X(\tau)$ | Dimensionless displacement |
| $x(t)$, $x(\tau)$ | Displacement, m |
| $Y_{1,2,3,4}$ | First derivative functions for Runge-Kutta method |

## References


Carnahan, B., Luther, H., & Wilkes, J. (1969). *Applied numerical methods*. New York, NY: John Wiley & Sons, Inc.

Erofeev, L., Smorodinov, M., Fedorov, B., Vyazovkii, V., & Villumsen, V. (1985). *Maschini i oborudanie dlya ustroiva osnovanii i fundamentov (machines and equipment for the installation of shallow and deep foundations)* (Second ed.). Moscow, Russia: Mashinostrenie.

Meriam, J. (1975). *Dynamics, si edition* (Second ed.). John Wiley & Sons, Inc.

Tseitlin, M., Verstov, V., & Azbel, G. (1987). *Vibratsionnaya tekhnika i tekhnologiya v svainykh i burovikh rabotakh (vibratory methods and the technology of piling and boring work)*. Leningrad, USSR: Stroiizdat, Leningradskoe Otdelenie.

Verstov, V., & Judina, A. (2015, January). Improving technological processes for borehole drilling in construction using vibration impact. *Applied Mechanics and Materials*, *725-726*, 220–225. doi: 10.4028/www.scientific.net/AMM.725-726.220

Warrington, D. C. (1992, October). Vibratory and impact-vibration pile driving equipment. *Pile Buck*(Second Issue), 2A–28A.

Warrington, D. C. (1994, August). Survey of methods for computing the power transmission of vibratory hammers. *Pile Buck*(Second Issue).

Warrington, D. C. (2006, September). Development of a parameter selection method for vibratory pile driver design with hammer suspension. *Colloquium of the Department of Mathematics of the University of Tennessee at Chattanooga*.

Warrington, D. C. (2021, April). *Reconstructing a soviet-era plastic model to predict vibratory pile driving performance* (Vol. 2021 ReSEARCH Dialogues Conference; Tech. Rep.). Chattanooga, TN: University of Tennessee at Chattanooga. doi: 10.13140/RG.2.2.30320.38403